Effects of Surface Dimples on Friction Coefficient of Reciprocating Model Lip Seals

L. LOU

In order to investigate the effect of surface dimples on the friction coefficient of a rod seal, model lip seals including six patterns of dimples and plane one were used to investigate the effect on friction coefficients. The differences of the friction coefficients between a plane model and models with dimples, and the effect of the specification of dimples are discussed. Furthermore, in order to explain the mechanism of the effect of dimples, the processes of oil film formation on the contact surface have been observed by an optical interferometric method. It was found that the effects of dimples on the friction coefficient could be explained by the oil film formation on the contact surface.

***Key Words**: dimple, rod seal, friction coefficient, oil film*

1. Introduction

Low sliding friction is one of the important factors for evaluating seal performance. An increased sliding resistance of a rod seal in a hydraulic power steering system causes a poor characteristic of steering feeling. In order to reduce the sliding resistance of the rod seal, it is required to reduce the seal's radial load or sliding friction coefficient. Various efforts[1), 2)] have been made to reduce the radial load for maintaining the sealing performance, for example, by reducing the spring tension or by reducing the contact area with maintaining the contact pressure. The reduction of sliding resistance by reducing the radial load has been already repeatedly performed and has substantially reached the limit. Thus, other types of efforts have been made to reduce the friction coefficient[3)~6)]. For example, a low friction material or a surface coating method by PTFE has been developed. However, these methods have a problem of increasing the cost of seals significantly. Therefore, in this research, it was tried to reduce the friction coefficient by designing micro-dimples on the contact surface.

2. Experimental Method

2. 1 Experimental Apparatus

A schematic diagram of an experimental apparatus is shown in **Fig. 1**. A model seal is attached between a glass disk and a load cell. The load applied to the model seal can be detected by the load cell. In order to simulate the reciprocating motion of the shaft, a servo motor is used to turn the glass disk. The oil film on the contact surface can be observed by a microscope. The measurement of the oil film was performed by an optical interferometric method[7)].

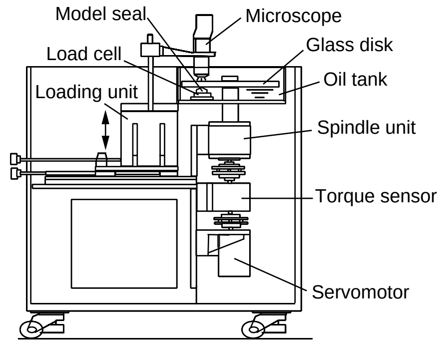

Fig. 1 Schematic diagram of experimental apparatus

2. 2 Model Seal and Dimple Pattern

Figure 2 shows the schematic diagram of a model seal. The micro-dimples were provided on the lip surface. In order to observe the influence of the micro-dimples, six types of dimple patterns shown in **Fig. 3** were designed, the specifications of which are shown in **Table 1**.

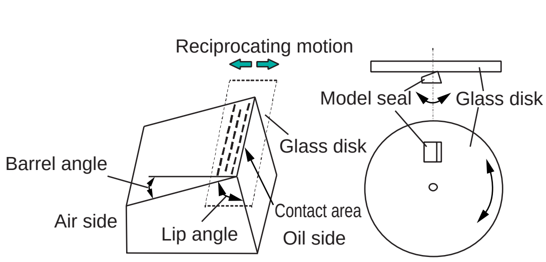

Fig. 2 Model seal

Table 1 Specifications of dimples

No.	Length, μm	Width, μm	Circumferential pitch, μm	Axial pitch, μm	Orientation angle of dimples, °	Depth, μm
1	180	30	340	160	0	30~40
2	180	100	340	160	0	
3	340	100	500	160	0	
4	340	100	680	320	0	
5	180	30	250	400	45	
6	340	100	410	400	45	
7	Without dimples					

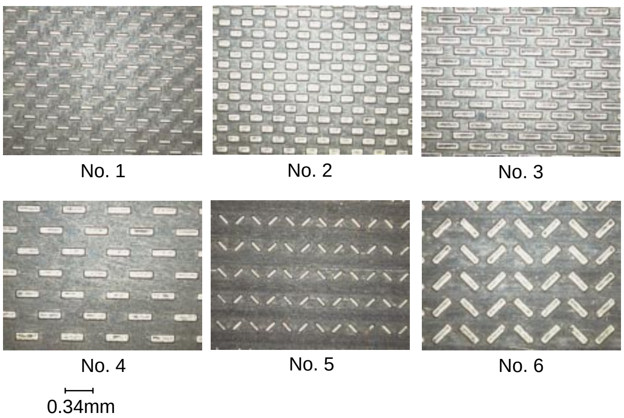

Fig. 3 Patterns of dimples

2. 3 Experimental Conditions

The experimental conditions are shown in **Table 2**.

Table 2 Experimental conditions

Material of model seal	Silicon rubber
Hardness, IRHD	55
Length of contact area, mm	30
Barrel angle, °	20
Temperature	Room temperature
Lubricant	Spindle oil (VG10)
Refractive index of oil	1.47
Load, N	32
Speed, mm/s	3, 5.9, 30, 59
Average rotating radius, mm	85

3. Results and Discussion

3. 1 In Case of Plane Model

3. 1. 1 Friction Coefficient Histories

Figure 4 shows the friction coefficient histories of a plane model obtained by the experiment under different speed conditions. In **Fig. 4**, positive friction coefficients were obtained when the glass disk was rotated in the clockwise direction while negative friction coefficients were obtained when the glass disk was rotated in the counterclockwise direction. As can be seen in **Fig. 4**, the positive friction coefficients rapidly increased at the beginning but subsequently declined toward the vicinity of the zero line. The negative friction coefficients increased with time and the maximum value appeared at the end of the process.

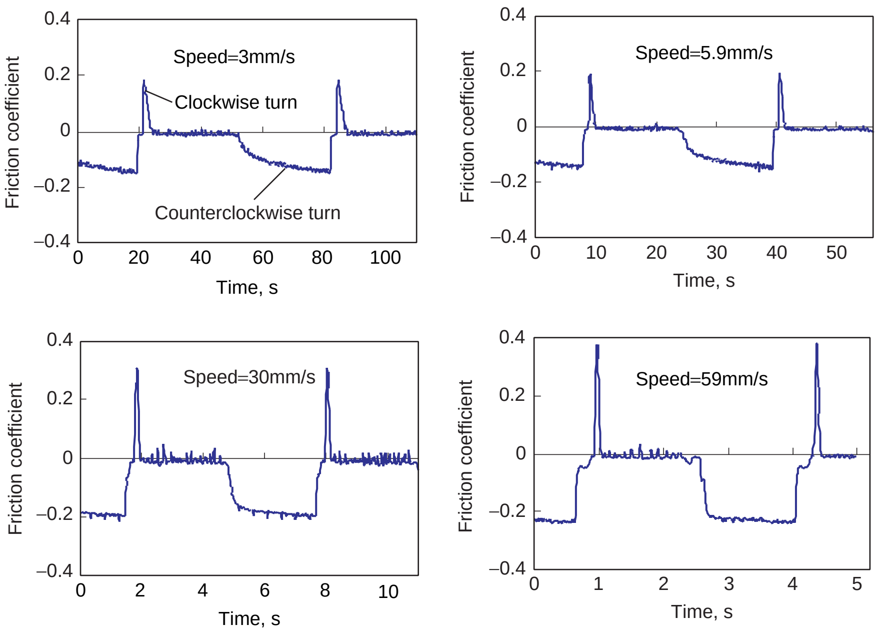

Fig. 4 Friction coefficient histories (plane model)

3. 1. 2 Formation of Oil Film

The reason why the peak of the positive friction coefficient appeared at the beginning of the process can be explained by the condition of the oil film formed on the contact surface. **Figure 5** shows how the oil film was formed on the contact surface with the speed of 59mm/s, where *t* represents the time during which the glass disk moves and the timing at which the oil film begins to be formed on the contact surface was determined to be zero. When the oil film is formed on the contact surface, interferograms will appear. When the model is in the static condition, interferograms were not observed on the contact surface. Thus, it can be assumed that the oil film was not formed on the contact surface. When the glass disk starts moving in the right direction, interferograms appeared on the contact surface. This means that the oil film started to be formed on the contact surface, which caused the decline of the friction coefficient as shown in **Fig. 4**. Under the conditions of **Fig. 5**, only about 0.09 second were required for the oil film to cover the entire contact surface. At the end of this process, the contact surface has thereon oil film having thickness of about 960 nm. What is notable here is that the time at which the oil film was formed on entire contact surface coincided with the time at which the peak of the positive friction coefficient as shown in **Fig. 4** appeared. This means that the appearance of the peak of the positive friction coefficient can be explained by the lubrication condition of the contact surface. **Figure 6** shows how the oil film having once been formed on the contact surface is removed from the contact surface of the plane model. As can be seen from **Fig. 6**, about 0.27 second were required for the oil film to be removed from the contact surface completely. The removal of the oil film in this process caused the friction coefficient of the contact surface to be increased and also caused the maximum friction coefficient to appear at the end of the process. This also caused the next process to allow the peak of the friction coefficient to appear at the start.

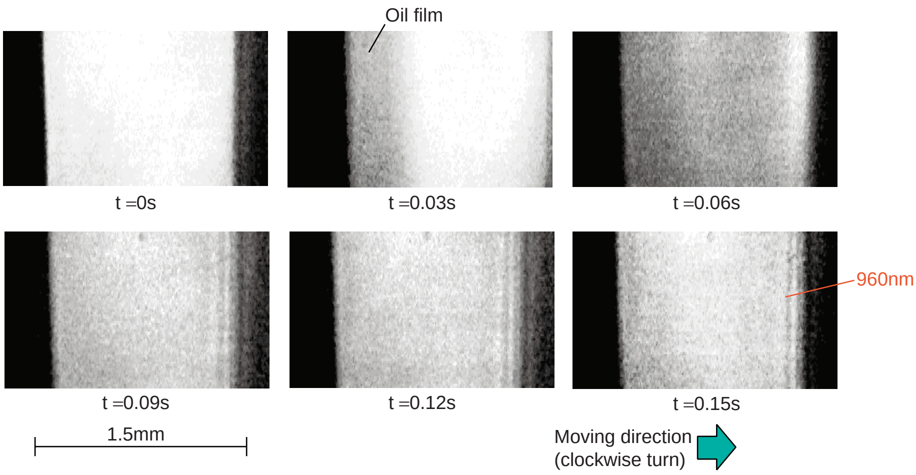

Fig. 5 Process of oil film formation (plane model, speed = 59mm/s)

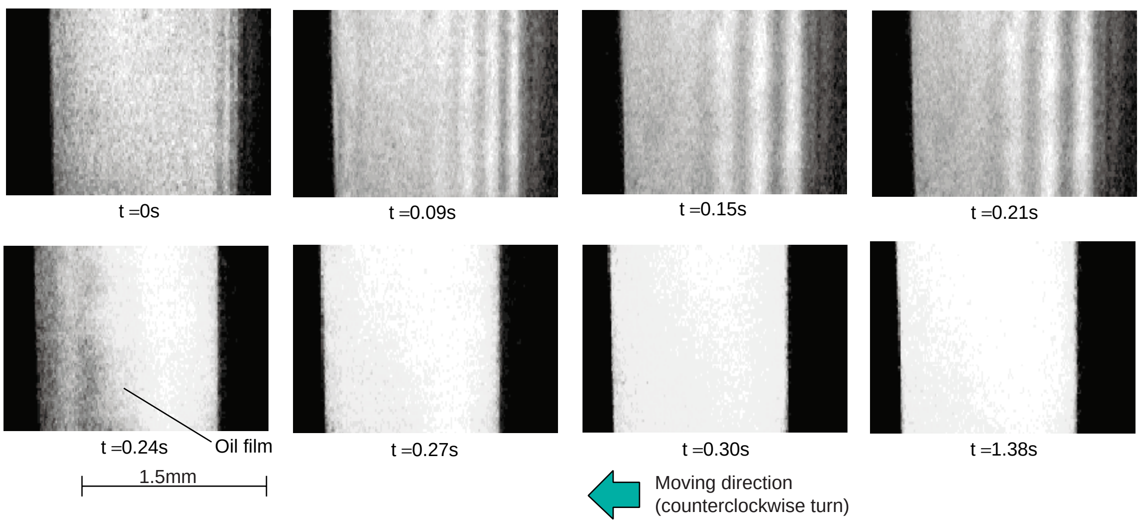

Fig. 6 Process of oil film removal (plane model, speed = 59mm/s)

3. 2 In Case of Dimple Model

3. 2. 1 Friction Coefficient Histories

Figures 7～10 show the friction coefficient histories of the six dimple models under different speed conditions. As is clear from the comparison between the friction coefficients shown in **Figs. 7～10** and those shown in **Fig. 4**, it is seen, at high speed, the maximum friction coefficient of a dimple model is significantly smaller than the maximum friction coefficient of a plane model. However, as the speed decreased, the maximum friction coefficient of the dimple model gradually increases as compared with the maximum friction coefficient of the plane model. This is a result by the fact that the reduced speed weakens the wedge effect between the model seal and the glass disk to reduce the amount of oil flow into the contact surface, preventing the oil film from forming on entire contact surface of the dimple model.

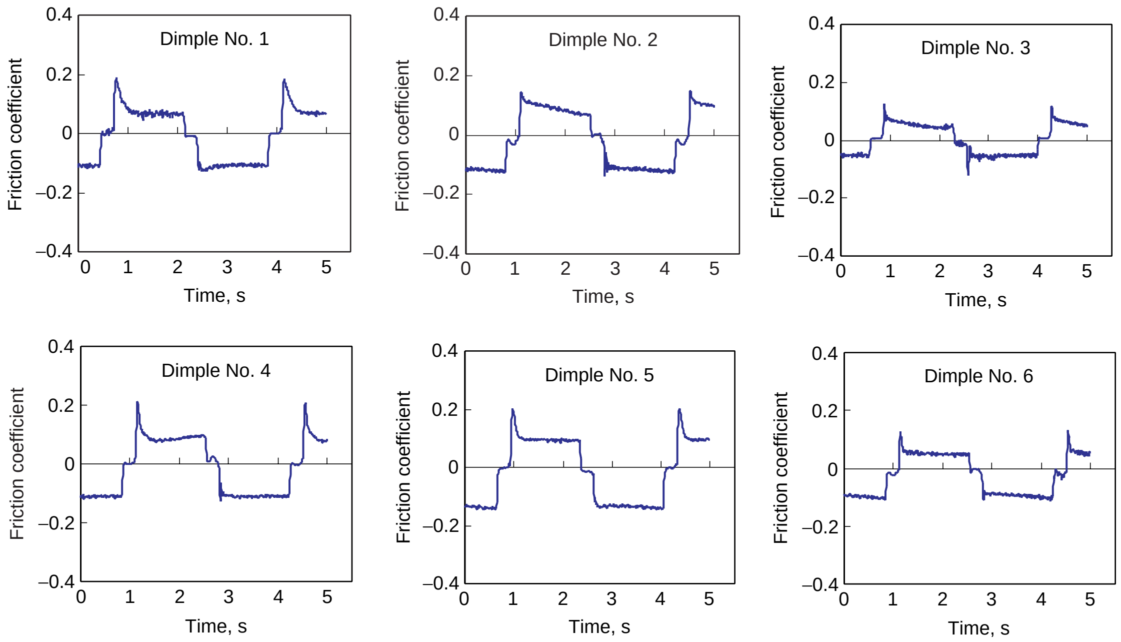

Fig. 7 Friction coefficient histories of dimple models (speed = 59mm/s)

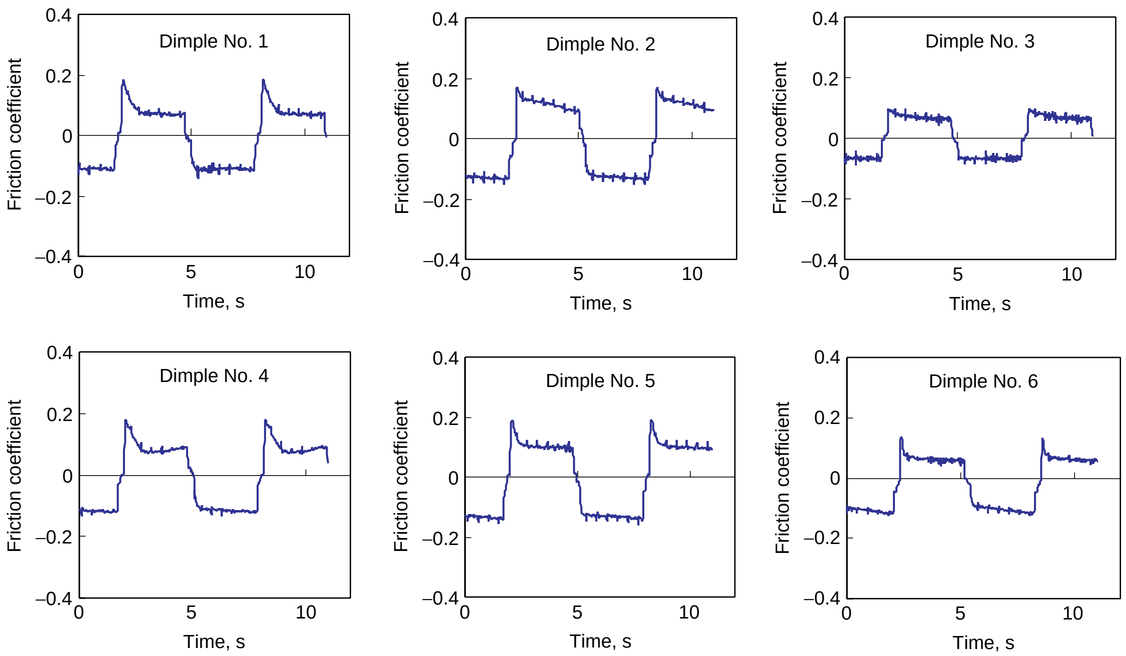

Fig. 8 Friction coefficient histories of dimple models (speed = 30mm/s)

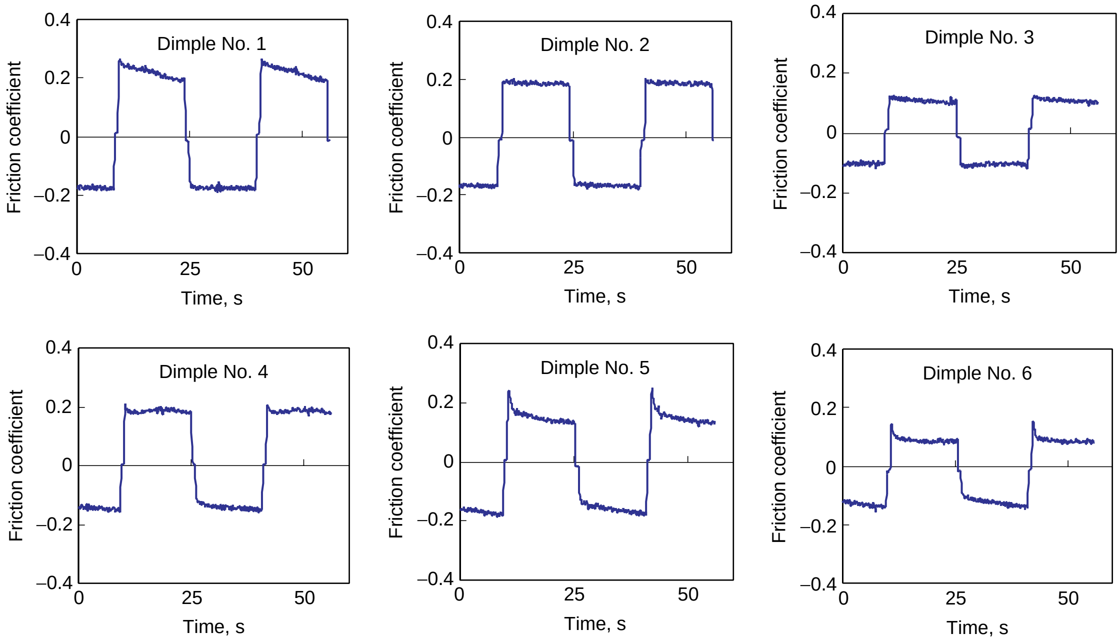

Fig. 9 Friction coefficient histories of dimple models (speed = 5.9mm/s)

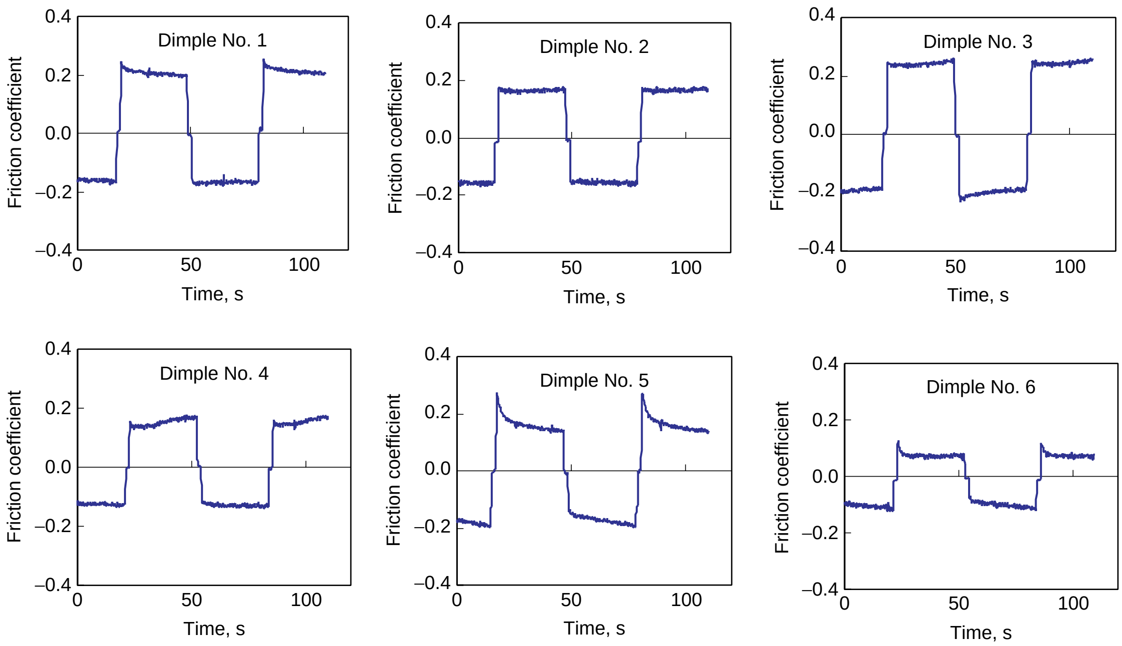

Fig. 10 Friction coefficient histories of dimple models (speed = 3mm/s)

3. 2. 2 Effect of Dimple Width and Length

When the results No. 1 and No. 2 shown in **Figs. 7～10** are compared, the influence by the dimple width on the friction coefficient can be understood. As can be seen from **Figs. 7～10**, those having larger dimple widths have relatively small friction coefficients.

Comparison between No. 2 and No. 3 shown in **Figs. 7～10** can provide the understanding of the influence by the dimple length on the friction coefficient. Also as can be seen from **Figs. 7～10**, those having a longer length of dimple have a relatively small friction coefficient.

Therefore, it can be said that a model having a longer length and wider width of a dimple has a smaller friction coefficient.

3. 2. 3 Effect of Dimple Orientation and Axial Pitch

When the results No. 4 and No. 6 shown in **Figs. 7～10** are compared, the influence by the dimple orientation on the friction coefficient can be understood. As can be seen from **Figs. 7～10**, No. 6 has relatively smaller friction coefficient as compared to that of No. 4. Thus, it can be understood that the dimple orientation also has an influence on the friction coefficient.

When the results No. 3 and No. 4 shown in **Figs. 7～10** are compared, the influence by the axial pitch of dimples can be understood. As can be seen from **Figs. 7～10**, No. 3 has a smaller friction coefficient as compared to that of No. 4. Thus, it can be understood that the dimple axial pitch has a significant influence on the friction coefficient. The smaller an axial pitch is, the smaller friction coefficient is.

3. 2. 4 Oil Film Formation

Figure 11 shows how oil film is removed from the contact surface of a dimple model. As can be seen from the comparison between **Fig. 11** and **Fig. 6**, a dimple model takes a longer time for oil film to be removed from the contact surface completely as compared to the case of a plane model. It only took about 0.27 second to remove the oil film from the entire contact surface in the plane model, while in the case of the dimple model, even at the end of the process (about 1.35 seconds), slight oil film still existed. In other words, the dimple model shows relatively longer lubrication time as compared to that of the plane model. This is why the dimple model has relatively smaller maximum friction coefficient.

Figure 12 shows an example of how the dimple model forms oil film on the contact surface. As can be seen from the comparison with the result of the plane model shown in **Fig. 5**, there exists a part of the contact surface not covered by the oil film in the dimple model. This is why the friction coefficients of the dimple models at the end of the process were larger than those in the plane model.

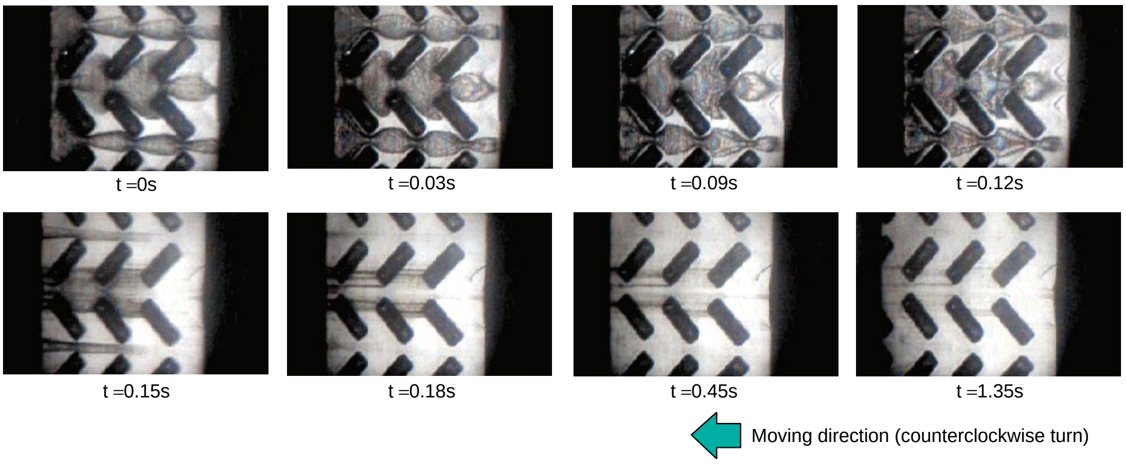

Fig. 11 Process of oil film removal (dimple model, speed = 59mm/s)

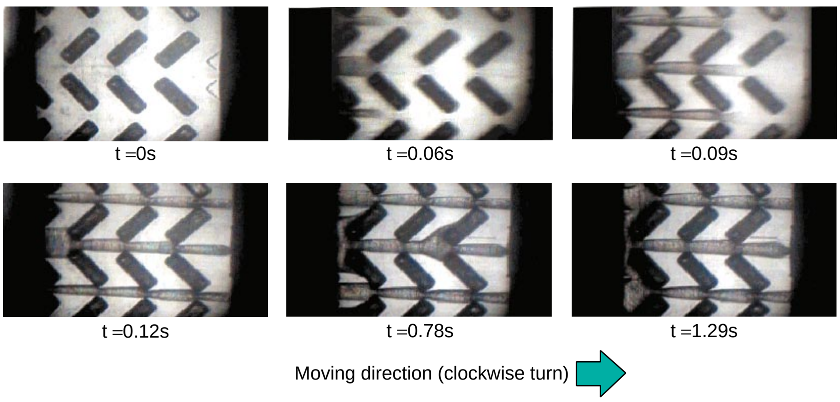

Fig. 12 Process of oil film formation (dimple model, speed = 59mm/s)

4. Conclusion

In order to investigate the influence on the friction coefficient by the micro-dimples provided on the contact surface, friction coefficients of the plane model seal and the six types of dimple model seals were measured. The processes of the oil film formation on the contact surface were observed by an optical interferometric method. As a result, the following findings were obtained.

1) The surface dimples have a large influence on the friction coefficient of the contact surface. Appropriate dimples can significantly reduce the maximum friction coefficient of the contact surface.
2) A dimple specification significantly changes the influence on the friction coefficient. This means the existence of an optimal dimple pattern. A dimple having a larger area and a smaller pitch gives relatively smaller friction coefficient.
3) Influence by dimples on the friction coefficient depends on the speed. The higher the speed is, the larger the influence is.
4) In the case of a plane model seal, the maximum friction coefficient increases with speed.

(This paper is an arranged version of the paper disclosed in the 17th International Conference on Fluid Sealing hosted by BHRG which was held in York, United Kingdom, 8～10 April, 2003.)

References

1) B. S. Nau : Proc. Instn. Mech. Engrs., vol. 213 Part J (1999) 215.
2) H. Yasui, T. Ojima, M. Mitsumaru: Koyo Engineering Journal, 127 (1985) 40.
3) F. Hirano, M. Kaneta: Proceedings of the Fifth BHRG International Conference on Fluid Sealing, 1971, paper G2 (BHRG Cranfield, Bedfordshire).
4) Y. Oki, M. Hirata, K. Ito: Tribologist (Journal of Japanese Society of Tribologists).
5) E. C. Bertolet: Proceedings of the 12th National Conference on Industrial Hydraulics, vol. 10 (1956) 56.
6) L. Lou: Proceedings of JAST Tribology Conference Tokyo (2001) 269.
7) L. Lou.: Lubrication Engineering (Dec. 2001) 15.
8) L. Lou.: Proceedings of the 17th International Conference on Fluid Sealing (2003) 187 (BHRG, York).

L. LOU*

* *Core Technology Research & Development Department, Research & Development Center, Dr.*